23rd International Conference
ENGINEERING MECHANICS 2017
Svratka, Czech Republic, 15 – 18 May 2017

# DYNAMIC CHARACTERISTICS OF PNEUMATIC ARTIFICIAL MUSCLES

**J. E. Takosoglu***

**Abstract:** *The article presents the test stand to determine the dynamic characteristics of pneumatic artificial muscles (PAM). Trigonometric dependencies occurring during the muscle operation were formulated. On the basis of the derived equations, a degree of the relative muscle contraction was calculated. The experimental research was conducted for two different masses affecting the pneumatic artificial muscles. The hysteresis of the muscle as well as dynamic characteristics for three different input signals were presented.*

**Keywords: Pneumatic artificial muscle, Dynamic characteristics, Proportional pressure valve, Pneumatornics.**

## 1. Introduction

Pneumatic artificial muscles are used mainly in drive systems of humanoid and anthropomorphic robots, bio-robots, exoskeletons and are more and more frequently applied in automation of production processes (Nowakowski et al., 2016a and Nowakowski et al., 2016b). Their application results from the advantages of pneumatic artificial muscles. The muscles are characterised by low mass, they generate greater forces in comparison with typical pneumatic cylinders with the same diameter, work smoothly even at a low speed, start and stop gently, a detrimental phenomenon of stick slip as well as the process of dry friction (Blasiak, 2016 and Blasiak et al., 2014) do not occur, they are completely hermetic and might operate in harsh and harmful environments (Laski et al., 2015 and Pietrala, 2016). Pneumatic artificial muscles are controlled by pressure changes in the muscle (Takosoglu, 2016). Proportional pressure valves or proportional flow valves are applied thereto the most frequently. An increase in the inner part of the muscle results in an increase of the muscle diameter (the muscle swells) and thus, the muscle is contracted and the pulling force is formed. The pulling force decreases from its max value (the muscle rests) to zero (the muscle is completely contracted). Fig. 1a shows an example of applying pneumatic artificial muscles in a bionic robot arm, whereas Fig. 1b presents an example of the application thereof in the vibrator of powdered materials.

a) 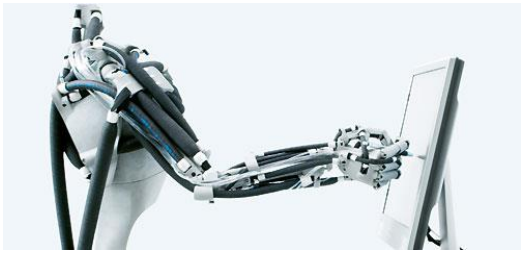 b) 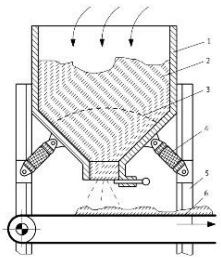

*Fig. 1: A bionic robot arm a), a vibrator of powdered materials b).*

## 2. Test stand

The test stand is built of stainless steel and its construction resembles scales (Bochnia, 2012). A centrally rotating arm was attached to an inverted T-shaped frame. At one end of the frame there is a pneumatic artificial muscle, whereas at the second one – load mass. Under the influence of the muscle contraction,

* BSc Jakub Emanuel Takosoglu, PhD.: Faculty of Mechatronics and Mechanical Engineering, Kielce University of Technology, Aleja Tysiaclecia Panstwa Polskiego 7, 25-314, Kielce; PL, qba@tu.kielce.pl

the arm rotates on two needle bearings, and the change of the rotational angle is registered by the angular position sensor. Fig. 2a presents a general diagram of the test stand, while Fig. 2b a general view of the test stand to determine the dynamic characteristics.

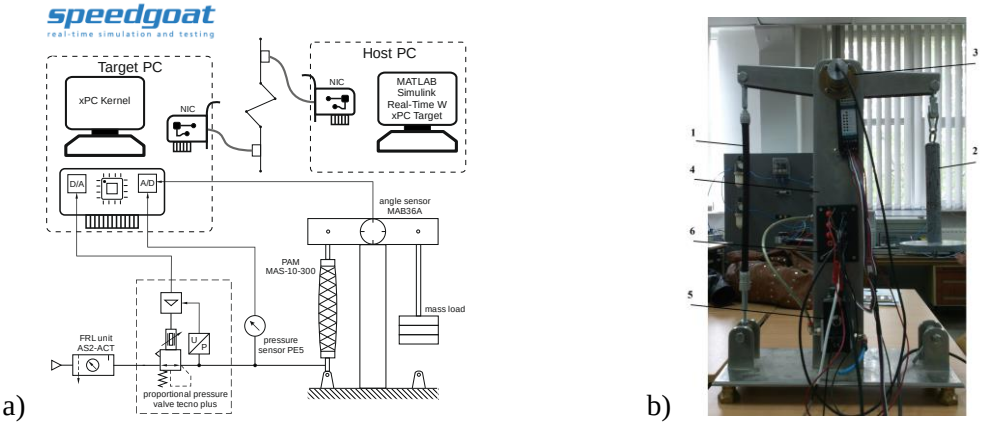


*Fig. 2: Test stand diagram a), general view of the test stand b).*

Piezoelectric proportional pressure value Hoerbiger Tecno Plus was applied to control the pneumatic muscle. The valve has a very short response time and low power consumption (Blasiak, 2016) (due to the piezoelectric transducer in the valve). An angular position sensor with an analog output, and a pressure sensor with an analog output were used in the measurement system (Adamczak et al., 2016 and Adamczak et al., 2015). The angular position sensor measures the rotational angle of the arm resulting from the muscle contraction. In order to collect the measurement and the valve control data, real time system Matlab and SpeedGoat hardware was applied (Dindorf, 2014 and Wos, 2015). The system consists of Intel Core 2 Duo 2.23 GHz CPU computer, 2048MB RAM, 1024MB industrial-grade CompactFlash device, 32 single-ended or 16 differential analog input (software selectable), 4 analog output (single-ended), and 8 digital TTL input and 8 digital TTL output channels (16-bit), I/O cable, terminal board. In order to determine the dynamic characteristics (Koruba, 2013 and Krzysztofik, 2014 and Grzyb, 2016 and Gapinski, 2014), the familiarity with the degree of the relative muscle contraction (contraction ratio) is crucial. In the measurement system, there is no direct measurement (Janecki, 2015) of the muscle contraction, that is why, trigonometric dependencies occurring during the muscle operation were formulated. Fig. 3a shows a diagram of trigonometric dependencies of the pneumatic muscle in the initial position, whereas Fig. 3b – during the muscle contraction.

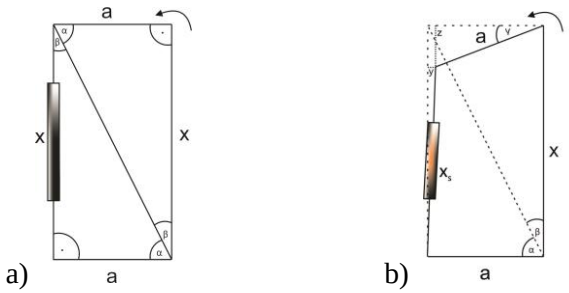


*Fig. 3: Diagram of trigonometric dependencies: a) at rest, b) during working.*

During the muscle contraction by $z$ value, $a$ arm rotates counter-clockwise, and in that way, acute angle $\gamma$ is formed (Fig. 5b). The following dependencies might be formulated on the basis of the diagram:

$$\alpha + \beta + (90^0 - \gamma) = 180^0 \tag{1}$$

$$\sin\gamma = \frac{z}{a} \tag{2}$$

$$\cos\gamma = \frac{a-y}{a} \tag{3}$$

$$x_s^2 = y^2 + (x - z)^2 \tag{4}$$

By substituting (1), (2) and (3) to equation (4), the length of the contracted pneumatic muscle was obtained:

$$x_s = \sqrt{(x - a \cdot \sin\gamma)^2 + (a - a \cdot \cos\gamma)^2} \tag{5}$$

It is important that static and dynamic characteristics be calculated using relative contraction of the muscle, also known as the contraction ratio (Takosoglu et al., 2016):

$$\varepsilon = \frac{L_n - x_s}{L_n} \cdot 100\ \% \tag{6}$$

where: $L_n$ – nominal length of the muscle,

$x_s$ – actual length of the muscle.

## 3. Experimental research

The pneumatic artificial muscle manufactured by Festo and marked as MAS-10-300 was applied in the experimental studies. The muscle parameters were included in Tab. 1.

*Tab. 1: Parameters of artificial pneumatic muscle MAS-10-300.*

| Parameter | Value |
|---|---|
| Symbol | MAS-10-300 |
| Mode of operation | *single-acting, pulling* |
| Internal diameter $D_n$ | *10 mm* |
| Nominal length $L_n$ | *300 mm* |
| Max. operating pressure $p$ | *0.8 MPa* |
| Max. permissible pre-tensioning $\varepsilon_{min}$ | *-2 % of $L_n$* |
| Max. permissible contraction $\varepsilon_{max}$ | *16 % of $L_n$* |
| Lifting force at max. permissible operating pressure $F_{max}$ | *630 N* |
| Max. additional load, freely suspended | *30 kg* |
| Operating frequency $f$ | *35 Hz* |
| Max. hysteresis | *3 % of nominal length* |
| Max. relaxation | *4 % of nominal length* |
| Repetition accuracy | *1 % of nominal length* |
| Ambient temperature | *-5 °C+60 °C* |

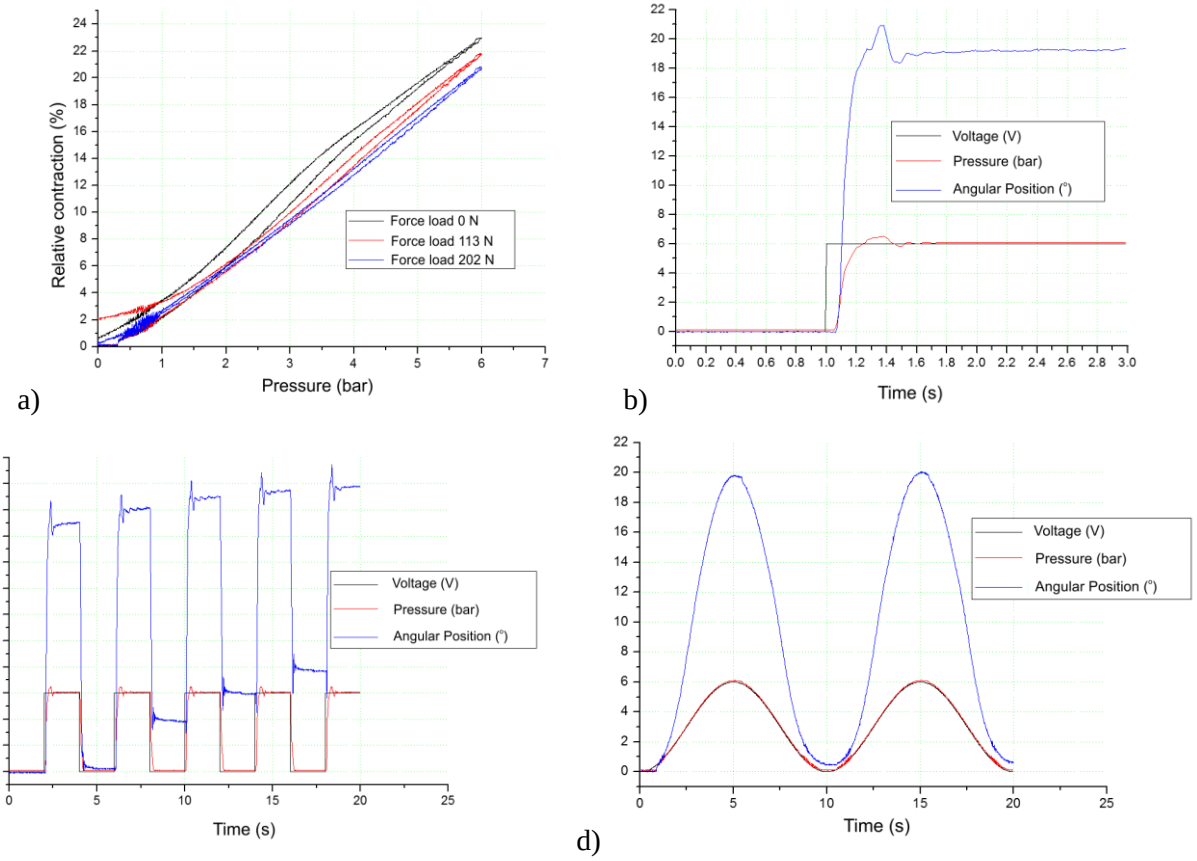


*Fig. 4: Relative muscle contraction in the pressure function a) dynamic characteristics of the muscle for three different control signals: b) step signal, c) rectangular signal, d) sinusoidal signal.*

Fig. 4a shows the obtained characteristics of the relative muscle contraction in the pressure function together with the hysteresis of the pneumatic muscle. Fig. 4b – 4d shows the dynamic characteristics of the pneumatic artificial muscle for three different control signals: step, rectangular and sinusoidal.

## 4. Conclusions

Taking the above research into consideration, it might be concluded that the hysteresis of MAS-10-300 pneumatic muscle is consistent with catalogue data and does not exceed 3 %. The repetition accuracy was verified for the rectangular control signal. The muscle performs 5 cycles (contraction – extension) within 20 sec. As it might be seen in the chart (Fig. 5b), the repetition does not exceed 1 %. The research was conducted with the max. pressure value of 0.6 MPa and for this pressure value, the degree of relative contraction reaches the max. value of 14 %. The designed test stand makes it possible to perform experimental studies of various types of pneumatic muscles.

## References


Adamczak, S., Zmarzly, P. and Janecki, D. (2015) Theoretical and practical investigations of v-block waviness measurement of cylindrical parts, Metrology and Measurement Systems, 22, 2, doi:10.1515/mms-2015-0023.

Adamczak, S., Zmarzly, P. and Stepien, K. (2016) Identification and analysis of optimal method parameters of the v-block waviness measurements, Bulletin of the Polish Academy of Sciences Technical Sciences, 64, 2.

Blasiak, M. (2016) Parametric analysis of piezoelectric transducer used for signal processing, in: Proc. 22th Int. Conf. Eng. Mech. 2016 (eds. Zolotarev, I. and Radolf, V.), Svratka, Czech Republic, pp. 66-69.

Blasiak, S., Takosoglu, J.E. and Laski, P.A. (2014) Heat transfer and thermal deformations in non-contacting face seals, Journal of Thermal Science and Technology, 9, 2, pp. 1-8, doi:10.1299/jtst.2014jtst0011.

Blasiak, S. and Zahorulko, A.V. (2016) A parametric and dynamic analysis of non-contacting gas face seals with modified surfaces, Tribology International, 94, , pp. 126-137, doi:10.1016/j.triboint.2015.08.014.

Bochnia, J. (2012) Ideal material models for engineering calculations, Procedia Engineering, 39, 0, pp. 98-110, doi:http://dx.doi.org/10.1016/j.proeng.2012.07.013.

Dindorf, R. and Wos, P. (2014) Contour error of the 3-dof hydraulic translational parallel manipulator, Advanced Materials Research, 874, pp. 57-62, doi:10.4028/www.scientific.net/AMR.874.57.

Gapinski, D. and Krzysztofik, I. (2014) The process of tracking an air target by the designed scanning and tracking seeker, in: Proc. 2014 15th Int. Carpathian Control Conf. IEEE, pp. 129-134.

Grzyb, M. and Stefanski, K. (2016) The use of special algorithm to control the flight of anti-aircraft missile, in: Proc. 22th Int. Conf. Eng. Mech. 2016 (eds. Zolotarev, I. and Radolf, V.), Svratka, Czech Republic, pp. 174-177.

Janecki, D. and Zwierzchowski, J. (2015) A method for determining the median line of measured cylindrical and conical surfaces, Measurement Science And Technology, 26, 8, doi:10.1088/0957-0233/26/8/085001.

Koruba, Z. and Krzysztofik, I. (2013) An algorithm for selecting optimal controls to determine the estimators of the coefficients of a mathematical model for the dynamics of a self-propelled anti-aircraft missile system, in: Proc. Institution of Mechanical Engineers, Part K: Journal of Multi-Body Dynamics, 227, 1, pp. 12-16.

Krzysztofik, I. and Koruba, Z. (2014) Mathematical model of movement of the observation and tracking head of an unmanned aerial vehicle performing ground target search and tracking, J. of Appl. Mathematics, 2014, pp. 1-11.

Laski, P.A., Takosoglu, J.E. and Blasiak, S. (2015) Design of a 3-dof tripod electro-pneumatic parallel manipulator, Robotics And Autonomous Systems, 72, pp. 59-70, doi:10.1016/j.robot.2015.04.009.

Nowakowski, L., Miesikowska, M. and Blasiak, M. (2016) Speech intelligibility in the position of cnc machine operator, in: Proc. 22th Int. Conf. Eng. Mech. 2016 (eds. Zolotarev, I and Radolf, V.), Svratka, Czech Republic, pp. 422-425.

Nowakowski, L., Miko, E. and Skrzyniarz, M. (2016) The analysis of the zone for initiating the cutting process of x37crmov51 steel, in: Proc. 22th Int. Conf. Eng. Mech. 2016 (eds. Zolotarev, I. and Radolf, V.) , Svratka, Czech Republic, pp. 426-429.

Pietrala, D.S. (2016) Parallel manipulator with pneumatic muscle drive, in: Proc. 22th Int. Conf. Eng. Mech. 2016 (eds. Zolotarev, I. and Radolf, V.), Svratka, Czech Republic, pp. 458-461.

Takosoglu, J.E. (2016) Control system of delta manipulator with pneumatic artificial muscles, in: Proc. 22th Int. Conf. Eng. Mech. 2016 (eds. Zolotarev, I. and Radolf, V.), Svratka, Czech Republic, pp. 546-549.

Takosoglu, J.E., Laski, P.A., Blasiak, S., Bracha, G. and Pietrala, D. (2016) Determining the static characteristics of pneumatic muscles, Measurement and Control, 49, 2, pp. 62-71, doi:10.1177/0020294016629176.

Wos, P. and Dindorf, R. (2015) Synchronized trajectory tracking control of 3-dof hydraulic translational parallel manipulator, in: Mechatronics - Ideas Ind. Appl. (eds. Awrejcewicz, J., Szewczyk, R., Trojnacki, M. and Kaliczynska, M.), Springer International Publishing, pp. 269-277, doi:10.1007/978-3-319-10990-9_24.